Int. J. Heat Mass Transfer. Vol. 30, No. 11, pp. 2357–2372, 1987
Printed in Great Britain

0017–9310/87 $3.00 + 0.00

Fluid flow and heat transfer in plasma reactors—I. Calculation of velocities, temperature profiles and mixing

A. H. DILAWARI† and J. SZEKELY
Department of Materials Science and Engineering, Massachusetts Institute of Technology, Cambridge, MA 02139, U.S.A.

(*Received* 10 *October* 1986 *and in final form* 13 *April* 1987)

Abstract—A mathematical representation has been developed to describe the velocity field and the associated temperature and concentration fields in a plasma jet system, which involves the injection of additional gas streams. In the statement of the problem, allowance was made for the swirl of the plasma jet, and one important objective of the work was to explore the effect of this swirl on the principal process variables. It was found that swirl plays an important role in providing mixing between the plasma jet and a reactant or diluent gas stream introduced through an annular port. It was shown, furthermore, that the model may be used for representing the quenching of the system by an axi-symmetrically introduced gas stream, having a direction perpendicular to the axis of the jet.

1. INTRODUCTION

RECENT studies have suggested that the synthesis of ceramics is perhaps the most promising application of thermal plasma technology [1–5]. In such processes, the ultimate objective is to obtain a monodispersed (or as close to monodispersed as possible) ceramic powder of micrometer or submicrometer size, through the reaction of suitable precursors. Possible examples include the production of silicon carbide or titanium diboride particles.

A schematic sketch of such a reaction system is given in Fig. 1, where an inert plasma jet, which is in essence the heat source, is brought into contact with one or more gaseous reactants—that is, the precursors. The design of the reactor is critical, because ideally:

(a) rapid reaction is to be achieved through good mixing of the plasma and precursors, such that many nuclei are being produced, but at the same time;
(b) the reaction system has to be quenched in order to prevent the agglomeration of the solid products.

In order to achieve these partially conflicting objectives, precise knowledge is required of mixing, and the velocity and temperature profiles in the system, together with appropriate causal relationships connecting these parameters to the system geometry, the location of the injection ports, and the like.

The purpose of this paper is to present computed results exploring the effect of:

(a) swirl;
(b) chamber size;
(c) injection arrangements;

on the temperature, on the velocity fields, and on the extent of mixing, which are the key parameters that govern reactor performance. These results will then be utilized in a subsequent paper, which will address the problem of decomposition and reaction kinetics.

One inherently unsatisfactory feature of numerical calculations is that the results are necessarily specific to the input parameters chosen. Furthermore, it would be quite impractical to present a large enough set of computed data so as to cover the range of process variables to be encountered in industrial practice. For this reason, we shall select computed results in order to provide insight regarding the sensitivity of the system to variations in process parameters, and note that the types of calculations presented here will have to be repeated in order to obtain design information for particular situations.

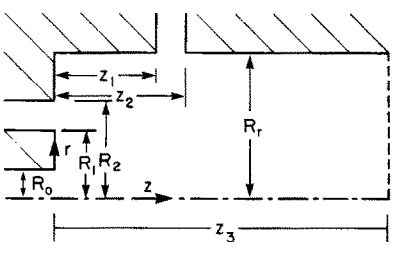

FIG. 1. A schematic sketch of a reaction system.

†A. H. Dilawari and J. Szekely are Visiting Associate Professor and Professor of Materials Science and Engineering, respectively. A. H. Dilawari is Associate Professor of Chemical Engineering, on leave from Institute of Chemical Engineering and Technology, Punjab University, Lahore 20, Pakistan.

NOMENCLATURE

C's	turbulence model constants
h	enthalpy
K	kinetic energy of turbulence
K_t	decomposition rate constant
m	mass fraction
P	pressure
P_w	power of the torch
Q_a	mass flow rate of annular stream of nitrogen
Q_l	mass flow rate of annular stream of silane
Q_m	mass flow rate of sideways stream of methane
Q_p	mass flow rate of argon plasma jet
Q_s	mass flow rate of sideways stream of nitrogen
r	radial coordinate
R_0	inside radius of the torch nozzle
R_r	radius of the reactor
T	temperature
T_{lw}	temperature of the left reactor wall
T_{tw}	temperature of the top reactor wall
T_t	temperature of the torch tip
u	axial velocity
u'	fluctuating component of axial velocity
v	radial velocity
v'	fluctuating component of radial velocity
w	azimuthal velocity
w'	component of azimuthal velocity
w_0	maximum azimuthal velocity at torch exit
z	axial coordinate.

Greek symbols

Γ	diffusion coefficient
ε	kinetic energy dissipation rate
η	thermal efficiency of the torch
θ	azimuthal coordinate
μ_e	effective viscosity
μ_l	laminar viscosity
μ_t	turbulent viscosity
ρ	density
σ's	Prandtl/Schmidt numbers for various transport quantities.

2. FORMULATION

Let us consider a cylindrical plasma jet issuing into a cylindrical chamber, as sketched in Fig. 1. In the system, provision is made also for the injection of two additional streams, one an annular jet and the other perpendicular to the axis of the plasma jet—while preserving cylindrical symmetry throughout. In the case considered here, the plasma gas will be considered to consist of argon, while the injected streams will be considered to consist of nitrogen. In the formulation, allowance may be made for swirl, so that three velocity components will have to be considered—axial, radial and azimuthal, while the independent variables are just two (the axial and the radial coordinates). The velocity and temperature distribution of the entering streams is considered to be known.

Then the mathematical statement of the problem is readily given by writing down:

(a) the equation of continuity;

(b) the three components of the equation of motion;

(c) the differential thermal energy balance equation;

(d) the differential mass conservation equation for a binary system;

(e) the K–ε model may be used to represent the turbulent viscosity and differential kinetic energy of turbulence and dissipation rate of turbulence equations proposed by Launder and Spalding [6].

The conservation equations of the axial, radial and azimuthal momentum components, the enthalpy, the mass concentration of individual species, the kinetic energy of turbulence and its dissipation rate can be written in general form—these transport equations are all similar—as follows:

$$\frac{1}{r}\frac{\partial}{\partial r}\left[r\left(\rho v\phi-\Gamma_\phi\frac{\partial\phi}{\partial r}\right)\right]+\frac{\partial}{\partial z}\left[\left(\rho u\phi-\Gamma_\phi\frac{\partial\phi}{\partial z}\right)\right]=S_\phi. \tag{1}$$

Here, ϕ is an index that may represent the velocity components, the enthalpy, or the mass concentration. Γ_ϕ and S_ϕ represent the corresponding transport coefficients and the source terms, respectively. If ϕ is set equal to unity and Γ_ϕ and S_ϕ to zero, this equation also represents the equation of continuity. These transport coefficients and the source terms are given in Table 1.

It should be remarked that in the statement of the energy balance equation, we postulated that the Lewis number is unity, so that the enthalpy transport due to concentration gradients is neglected. This assumption is usually made in combustion studies and is thought to be particularly applicable to turbulent conditions [7–10].

2.1. *Swirl number*

The degree of swirl is normally represented by the swirl number, defined as

$$S'=\frac{G_\theta}{G_z R_0} \tag{2}$$

Table 1. The transport coefficients and source terms

Variable ϕ	Γ_ϕ	S_ϕ
1	0	0
u	$\mu_e = \mu_l + \mu_t$	$-\frac{\partial P}{\partial z} + \frac{1}{r}\frac{\partial}{\partial r}\left(r\mu_e \frac{\partial v}{\partial z}\right) + \frac{\partial}{\partial z}\left(\mu_e \frac{\partial u}{\partial z}\right)$
v	μ_e	$-\frac{\partial P}{\partial r} - \frac{2\mu_e v}{r} + \frac{1}{r}\frac{\partial}{\partial r}\left(r\mu_e \frac{\partial v}{\partial r}\right) + \frac{\rho w^2}{r} + \frac{\partial}{\partial z}\left(\mu_e \frac{\partial u}{\partial z}\right)$
rw	μ_e	$-\frac{2}{r}\frac{\partial}{\partial r}(\mu_e rw)$
K	μ_e/σ_K	$G-\rho\varepsilon$
ε	μ_e/σ_ε	$\frac{\varepsilon}{K}(C_1 G - C_2\varepsilon)$
h	μ_e/σ_h	$-S_R$
m	μ_e/σ_m	0

Notes:
(1) $\mu_t = C_D \rho K^2/\varepsilon$.
(2) Turbulence model constants are assigned the following values:

$$C_D = 0.09, \quad C_1 = 1.43, \quad C_2 = 1.92,$$
$$\sigma_K = 1, \quad \sigma_\varepsilon = 1.22, \quad \sigma_h = \sigma_m = 0.9.$$

(3) $G = \mu_e\left[2\left(\frac{\partial u}{\partial z}\right)^2 + 2\left(\frac{\partial v}{\partial r}\right)^2 + 2\left(\frac{v}{r}\right)^2 + \left(\frac{\partial w}{\partial r} - \frac{w}{r}\right)^2 + \left(\frac{\partial w}{\partial z}\right)^2 + \left(\frac{\partial u}{\partial r} + \frac{\partial v}{\partial z}\right)^2\right]$.

where

$$G_\theta = \int_0^\infty (\rho uw + \rho\overline{u'w'})r^2\,dr \tag{3}$$

is the axial flux of angular momentum, including the z–θ direction turbulent shear stress term and

$$G_z = \int_0^\infty (\rho u^2 + \rho\overline{u'^2} + (P - P_\infty))r\,dr \tag{4}$$

is the axial flux of axial momentum, including the z-direction turbulent normal stress term, and a pressure term.

When the solid body plug flow is assumed at the nozzle, i.e. the axial velocity is flat and w increases from zero at $r = 0$ to w_0 at $r = R_0$, then local static pressure P and swirl velocity w are related as

$$P - P_\infty = -\tfrac{1}{2}\rho w^2 \tag{5}$$

where P_∞ is static absolute pressure at $r = R_0$ and $z = 0$.

If the turbulent stress terms are omitted and density is assumed constant implying a flat temperature profile at the inlet plane, one may readily obtain

$$S' = \frac{(w_0/2u_0)}{1-(w_0/2u_0)^2} \tag{6}$$

and

$$S = w_0/2u_0 \tag{7}$$

if pressure is omitted in G_z. Both S and S' are called swirl numbers. In the present work, equation (7) is used to represent the degree of swirl. It may, however, be pointed out that for higher degrees of swirl the axial velocity distribution deviates from plug flow considerably—the major portion of the flow leaves the nozzle near the outer edge [11, 12] and the measured value of swirl number differs from the value obtained from equation (6) using measured values of velocities [12].

2.2. *Boundary conditions*

The governing equations are elliptic, which requires that boundary conditions be given for all boundaries. At the inlet plane for both the argon plasma jet and the annular nitrogen jet, profiles for the axial velocity, temperature, mass concentration of argon and nitrogen, kinetic energy of turbulence and turbulence dissipation rate are considered to be flat. The radial velocity v, for both the plasma jet and the parallel annular jet, was given a zero value. The swirl velocity profile for the plasma jet is assumed to be that of a solid body rotation. In a certain sense, axial and swirl velocity conditions are arbitrary, but it is believed that the swirl number and the average velocity are the important features of the inlet profiles. Values for K and ε were obtained using relations proposed by Pun and Spalding [13].

For the sideways stream, u, rw, K, ε, and m were assigned zero value, while a uniform profile for the radial velocity was used.

At the wall boundaries, the normal velocity is set to zero, while near-wall tangential velocities are connected with their zero wall values by way of the wall functions [6].

The effect of swirl on wall function specification is handled by extending the previous ideas. The velocity is the total tangential velocity and is non-dimensionalized with respect to the total tangential shear stress. The appropriate expressions are then deduced for tangential velocity components. The effects on momentum equations are incorporated via the usual linearized source technique. The total tangential shear stress is formulated by observing that convection and diffusion of turbulent kinetic energy are negligible in this region [14] and that isotropic viscosity holds true. Also, in arriving at the final expression for the top wall diffusion flux for the z-momentum equation, it is assumed that $\partial v/\partial z$ approaches zero near the top wall [15]. Further, the gradient of turbulent kinetic energy was set to zero, and its dissipation rate was calculated assuming an equilibrium boundary layer.

The smooth wall boundary condition formula for h proposed by Launder and Spalding [6] is employed using the total tangential shear stress. As for mass concentration m, mass flux equal to zero is employed. A similar analysis was made for the tip of the torch and the left wall of the reactor.

At the centerline, the gradients of u, K, ε, rw, and m are zero, while the radial velocity v is zero. At the reactor exit, the flow is assumed to be fully developed, i.e. the radial velocity and the gradients of all the remaining transportable quantities are set to zero.

The standard two-equation K–ε turbulence model is employed, which has been used in a wide variety of turbulent flow situations, and good predictive capability has been achieved. It is generally thought that the K–ε turbulence model is in need of improvement for adequate simulation of the turbulent swirling recirculating non-isothermal flow in question. While these arguments are readily accepted, it is suggested that such a refinement will be best undertaken when comprehensive experimental measurements become available.

2.3. *Solution procedure*

The basic 2/E/FIX computer program [13] provides the starting point from which the present computer program has been developed. The procedure is based on the finite volume approach, with diffusion approximated by central difference and convection modelled through an upwind difference. For the general variable ϕ, the partial differential equation is represented by a coupled set of algebraic equations of the form

$$A_P\phi_P = \Sigma A_i\phi_i + S_{\phi,P}, \quad i = N, S, E, W \qquad (8)$$

where P, N, S, E, W denote mesh nodes and $S_{\phi,P}$ is the source term in the equation.

The method of solution adopted followed the 'SIMPLE' procedure [16, 17], which essentially involved several iterative cycles; initial estimates were made of the velocity, temperature, concentration and pressure fields, and the density and transport coefficients were calculated.

The second iterative loop involved the re-calculation of the primary variables and the same procedure was repeated until satisfactory convergence was obtained. An additional important convergence criterion was that the mass balance had to be satisfied to within $\pm 0.5\%$.

The computational mesh used for all calculations consisted of 27×30 non-uniformly distributed grid points with a high gridline concentration close to the torch exit where variations of all variables are expected to be highest. A typical run to reduce momentum and mass sources to below 0.5% of the inlet values required 600 iterations and computer (cpu) time was of the order of 1 h of MicroVAX II. The cpu time increased to 1.5 h for a thermal decomposition of silane using methane as an inert quench gas, in which case additional transport equations for mass concentration of silane and hydrogen were solved; a typical run required 800 iterations.

Other useful designer information, like streamline plots showing recirculation zones and stagnation points, is easily produced. Streamline plots are obtained for the dimensionless stream function, which is given by

$$\psi^* = \int_0^r \rho ur\,\mathrm{d}r \Big/ \int_0^{R_0} \rho ur\,\mathrm{d}r. \qquad (9)$$

3. COMPUTED RESULTS

In the following, we shall present a selection of the computed results. In essence, the following specific cases will be considered.

(1) The behavior of a coaxial jet, both in the absence and presence of swirl.

(2) The behaviour of a coaxial jet with sideways injection.

In selecting these cases and the input parameters, our aim was to provide general insight regarding behavior of these systems, with emphasis on the sensitivity to given process parameters. In operating plasma reactors for the synthesis of fine, monodispersed ceramic particles, two important objectives must be achieved:

(a) the reactants have to be heated rapidly to the reaction temperature and well mixed (in the case of complex reaction systems);

(b) the products have to be rapidly quenched, so as to minimize agglomeration and growth of the fine particles produced in the reaction zone.

It is the aim of the computed results, to be presented subsequently, to illustrate that by imposing swirl and through the suitable location of ports for introducing the quench gas, one may achieve these objectives. The

Table 2. Input parameters used

$P_w = 37\,\text{kW}$
$Q_a = 6.0 \times 10^{-3}\,\text{kg s}^{-1}$
$Q_p = 1.69 \times 10^{-3}\,\text{kg s}^{-1}$
$Q_s = 9.5 \times 10^{-2}\,\text{kg s}^{-1}$
$R_0 = 0.005\,\text{m}$
$R_1 = 0.0075\,\text{m}$
$R_2 = 0.01\,\text{m}$
$R_r = 0.0125\,\text{m}$
$T_{lw} = 0.6\,\text{kK}$
$T_{tw} = 0.6\,\text{kK}$
$T_t = 0.6\,\text{kK}$
$z_1 = 0.053\,\text{m}$
$z_2 = 0.1075\,\text{m}$
$z_3 = 0.40\,\text{m}$
$\eta = 62\%$

'standard' input parameters used in these calculations are summarized in Table 2. The property values used in the calculations were taken from the tabulated data of Liu [18] and that of Yos [19]. In essence, the mass flow rate of the annular stream was three times that of the plasma jet, while the quench gas flow rate was some 60 times that of the plasma stream.

Figures 2(a)–(d) show the computed results for a non-swirling plasma jet, which can be regarded as the 'standard case', here Fig. 2(a) gives the velocity field, Fig. 2(b) is the temperature field, Fig. 2(c) is the map of the argon concentration, and Fig. 2(d) is the streamline pattern. It is seen that mixing is relatively slow and that the high temperature region extends to the substantial length of the reactor.

It is of interest to contrast these plots to those shown in Figs. 3 and 4, for identical conditions, but for a swirl number of 0.5 and 1, characterizing the argon jet. The very complex velocity field, with reverse flow near the center, is readily apparent; as a result of the swirl, the temperature profiles are markedly modified, and mixing of the argon and the nitrogen streams is promoted.

The following set of figures depicts the effect of injecting a nitrogen stream through a port, in the chamber, in a direction perpendicular to the axis of the jet. As seen in Table 2, the mass flow rate of this stream is some 60 times that of the plasma gas. Such an arrangement would be appropriate if the objective were to quench the system, e.g. after the completion of a reaction step, in order to prevent either a reverse reaction or to prevent the agglomeration of the fine particles produced.

Here, Fig. 5(a) shows the computed velocity field in the absence of swirl, where it is seen that the impact of the sideways-injected stream is considerable. Figures 5(b) and (c) show the effect of employing a swirl number of 0.5 and 1, respectively. It may be observed that while a swirl number of 0.5 does modify the velocity field for the conditions employed, actual flow reversal will take place in the region of a swirl number of unity. The very complex velocity field observed in Fig. 5(c) will be highly conducive to mixing, as will be seen subsequently. It should be remarked here that the high value of the swirl number required in order to bring about flow reversal is due to the fact that the incoming plasma jet is at a very high temperature, so that its density is necessarily low. Since the density appears in the momentum balance, identical swirl numbers will have a significantly lesser effect for systems with a hot plasma jet discharging into a cold environment than for an isothermal situation.

Figures 6(a)–(c) show the argon concentration maps for sideways injection and for progressively increasing swirl numbers. The greatly increased mixing brought about by the swirl is readily apparent here. One should recall here that in the absence of swirl, the effect of the sideways injection will be manifested only downstream from the injection port. When swirl is introduced, its effect will be twofold: one, it will promote mixing with the annular jet—the prin-

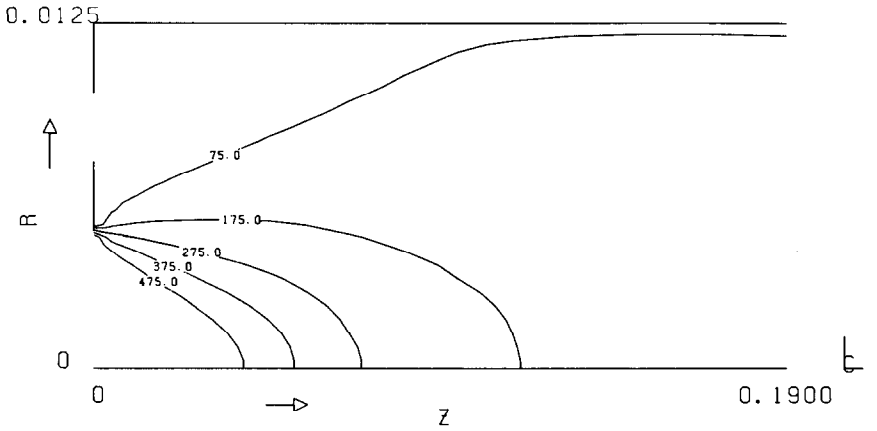

FIG. 2(a). Computed axial velocity field for no sideways injection and $S = 0$.

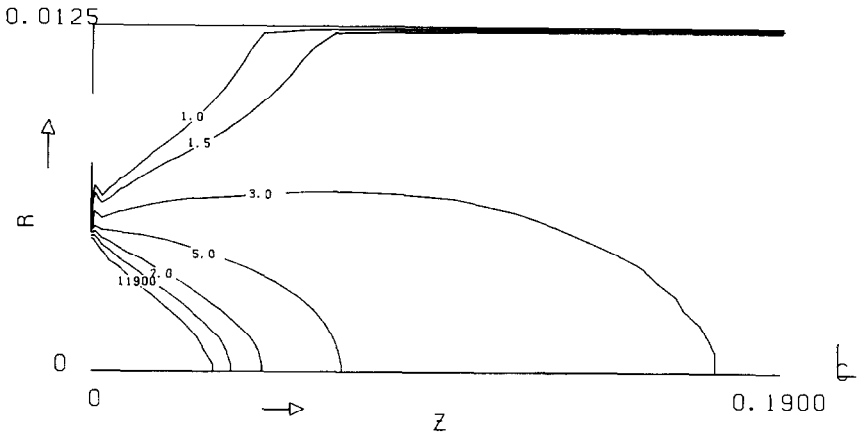

FIG. 2(b). Computed isotherms for no sideways injection and $S = 0$.

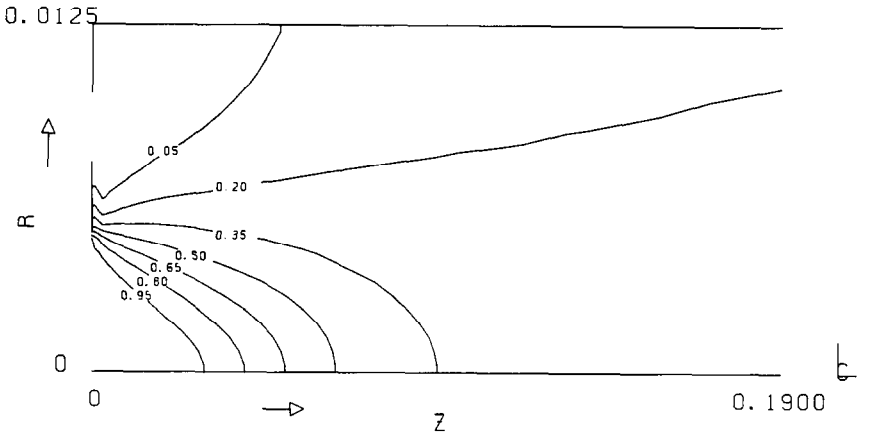

FIG. 2(c). Computed map of argon concentration with no sideways injection and $S = 0$.

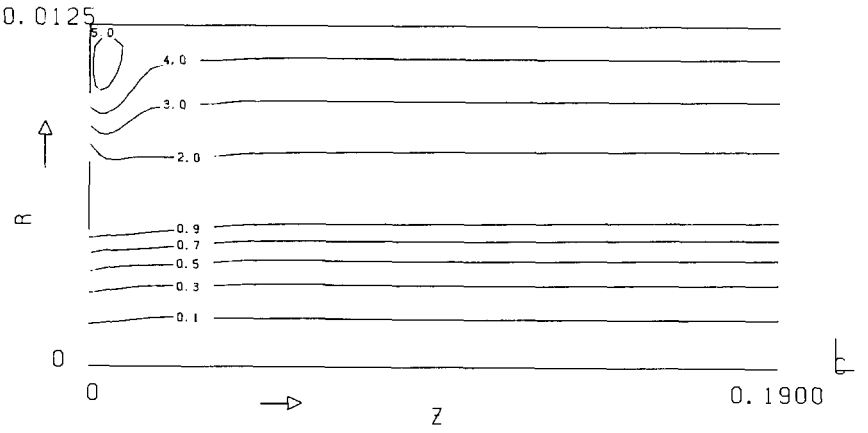

FIG. 2(d). Computed streamline pattern with no sideways injection and $S = 0$.

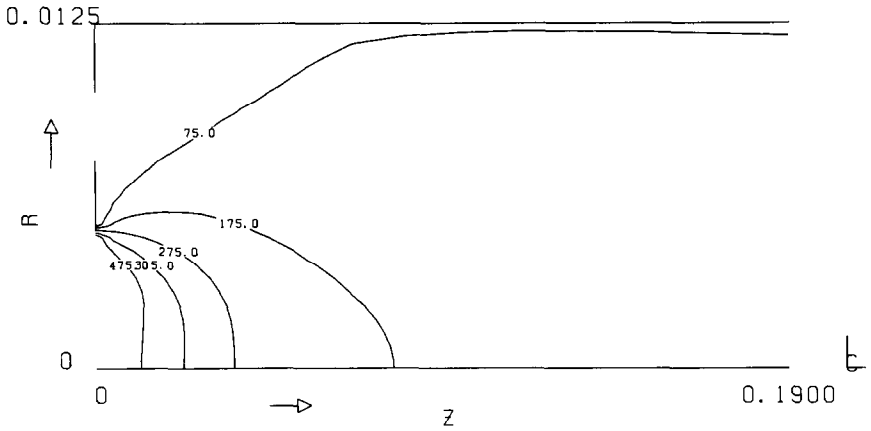

FIG. 3(a). Computed axial velocity field for no sideways injection and $S = 0.5$.

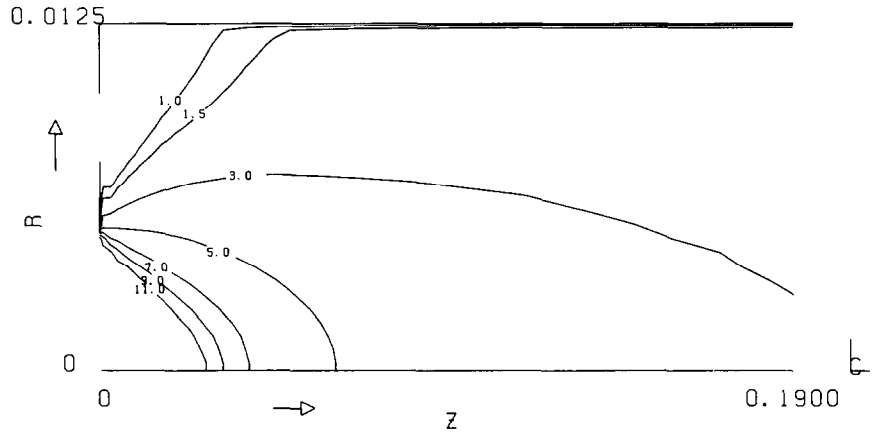

FIG. 3(b). Computed temperature profiles for no sideways injection and $S = 0.5$.

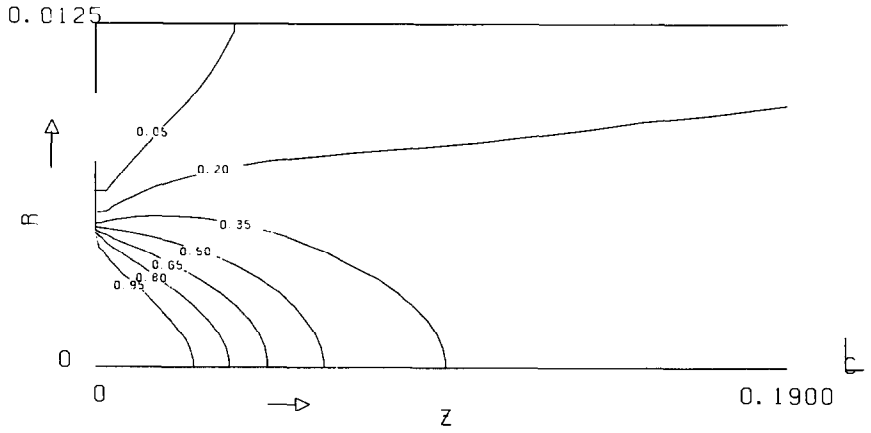

FIG. 3(c). Computed map of argon concentration for no sideways injection and $S = 0.5$.

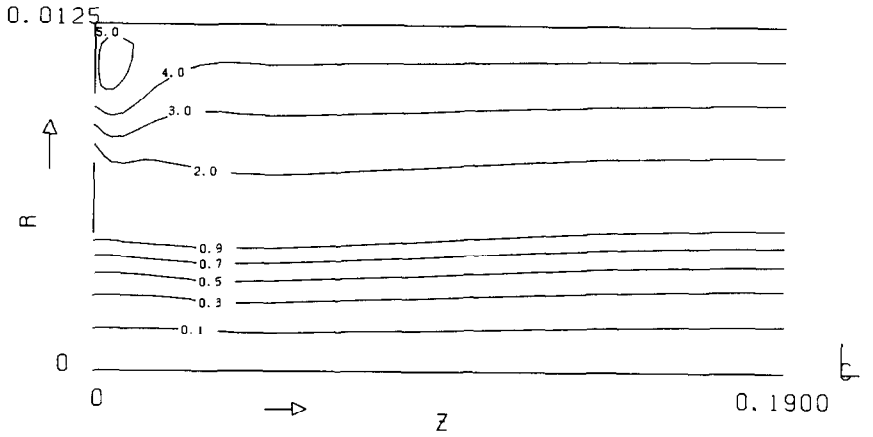

FIG. 3(d). Computed streamline pattern for no sideways injection and $S = 0.5$.

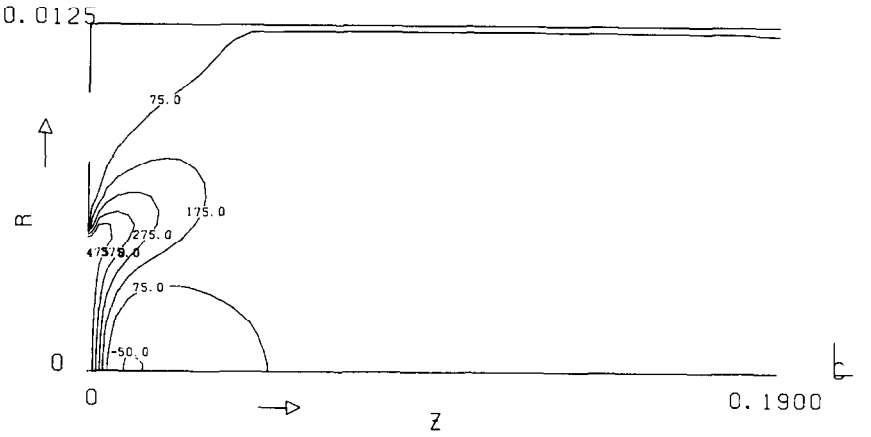

FIG. 4(a). Computed axial velocity field for no sideways injection and $S = 1$.

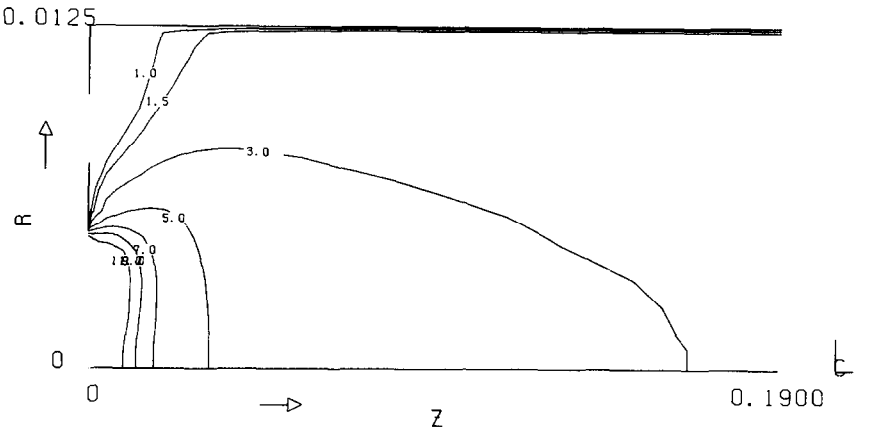

FIG. 4(b). Computed isotherms for no sideways injection and $S = 1$.

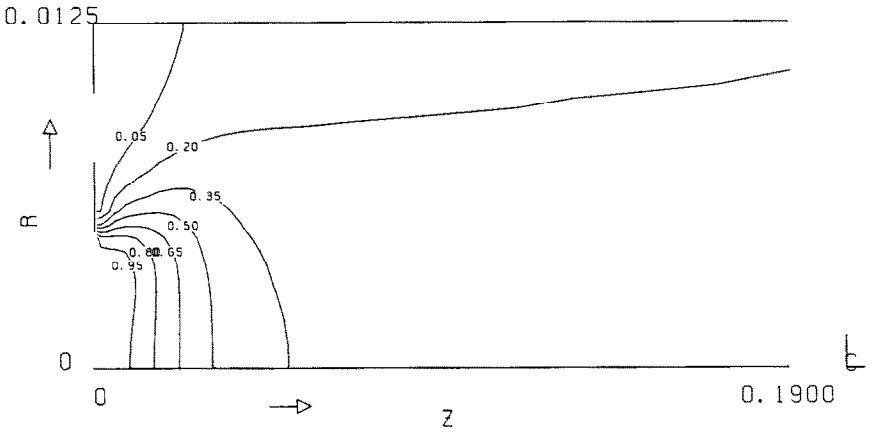

FIG. 4(c). Computed map of argon concentration with no sideways injection and $S = 1$.

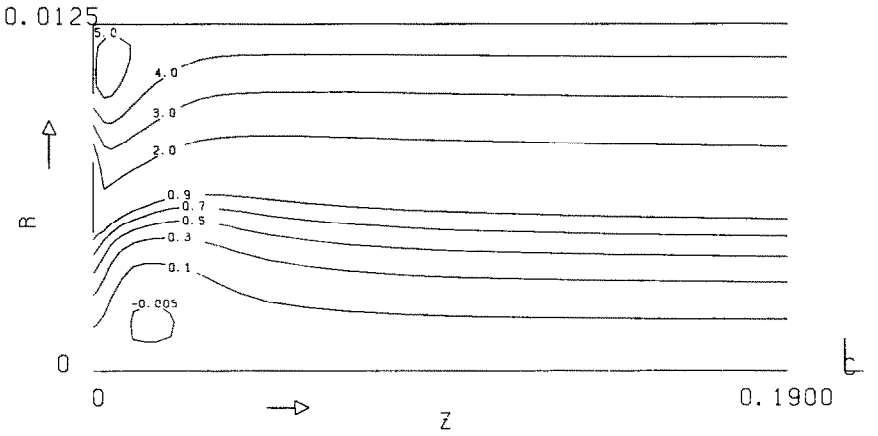

FIG. 4(d). Computed streamline pattern for no sideways injection and $S = 1$.

cipal effect; also, it will enhance the interaction with the sideways-injected stream.

Figures 7(a)–(c) show the corresponding temperature fields with sideways injection, again with increasing swirl numbers. Inspection of these figures shows that the plasma jet may be effectively quenched by sideways injection, but that this quenching effort is markedly enhanced by the presence of swirl. More specifically, the position of the 3 and 5 kK contours, which define the effective reaction zones for many applications, are markedly modified.

If somewhat arbitrarily, we define an 'effective reaction zone' such that the argon content is higher than, say, 20%, and the temperature higher than, say, 3 kK. It is readily seen from the figures previously given that by adjustment of the swirl number, one can change the size of the reaction zone and, hence, the reaction characteristics of the system. Calculations that have been carried out (but are not reproduced here) indicate that, in a similar vein, one can markedly modify the size of the reaction zone by adjusting the volumetric flow rates of the annular and quench gas streams.

An alternative way of representing the velocity field is through the streamline patterns, as done in Figs. 8(a)–(c). The dominant effect of the sideways-injected stream is readily apparent on these plots, as is the manifestation of the reverse flow once a swirl number of unity is approached.

Additional calculations have been carried out which are not reproduced here, to examine the effect of the chamber size, the effect of changing the location of the annular port, and also changing the angle of injection of the annular gas stream; furthermore, we also examined the effect of changing the position of the port through which the side stream was injected. In a sense, the results followed the 'expected pattern'. The radial location of the annular stream had a much less pronounced effect than swirl in affecting mixing, although the position of the annular port will be an important design factor.

As an illustration, Fig. 9 shows the computed argon

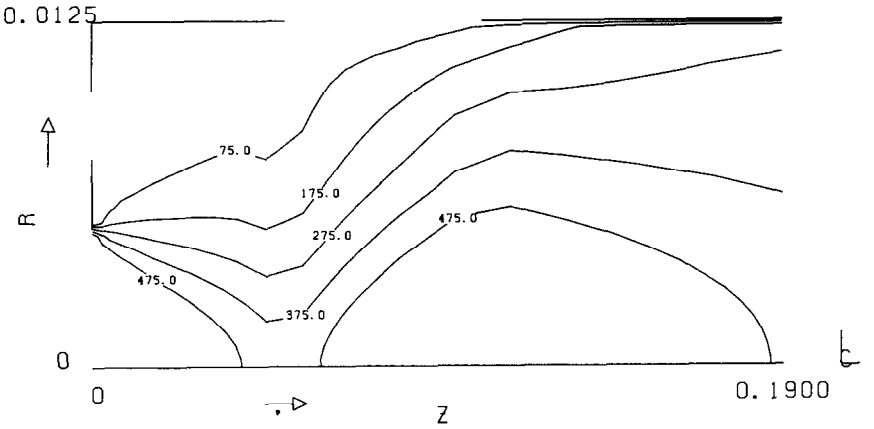

FIG. 5(a). Computed axial velocity field for sideways injection and $S = 0$.

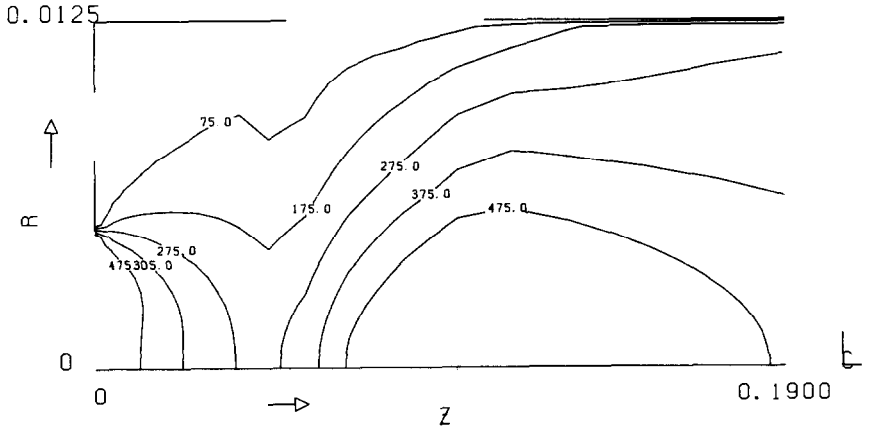

FIG. 5(b). Computed axial velocity field for sideways injection and $S = 0.5$.

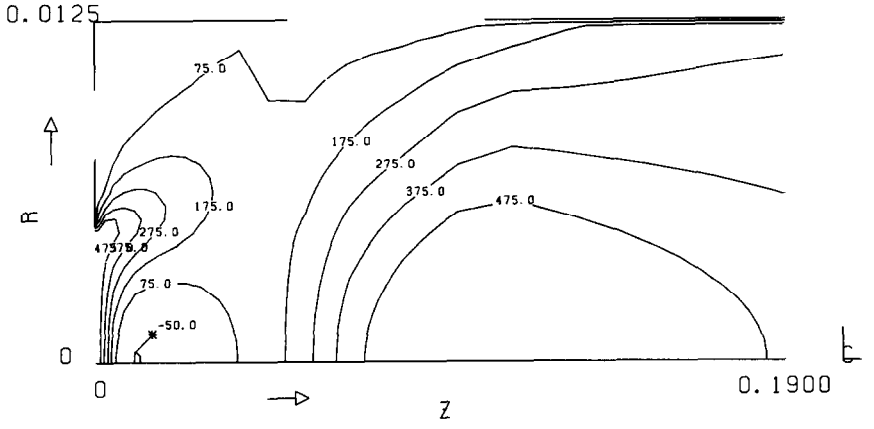

FIG. 5(c). Computed axial velocity field for sideways injection and $S = 1$.

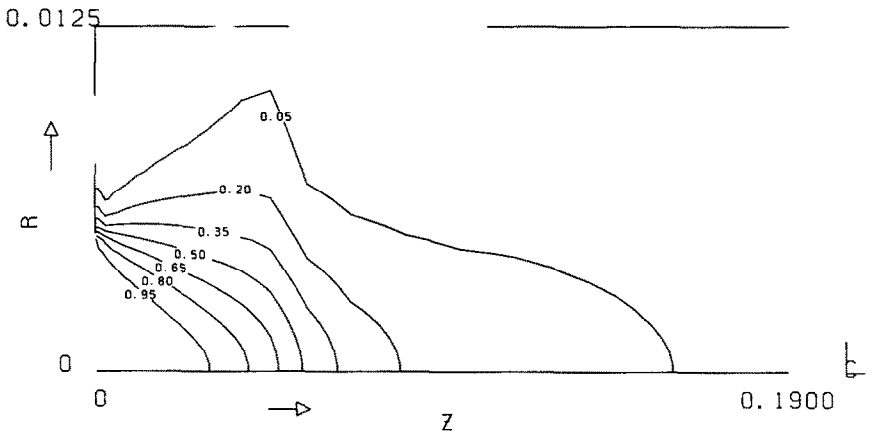

FIG. 6(a). Computed map of argon concentration for sideways injection and $S = 0$.

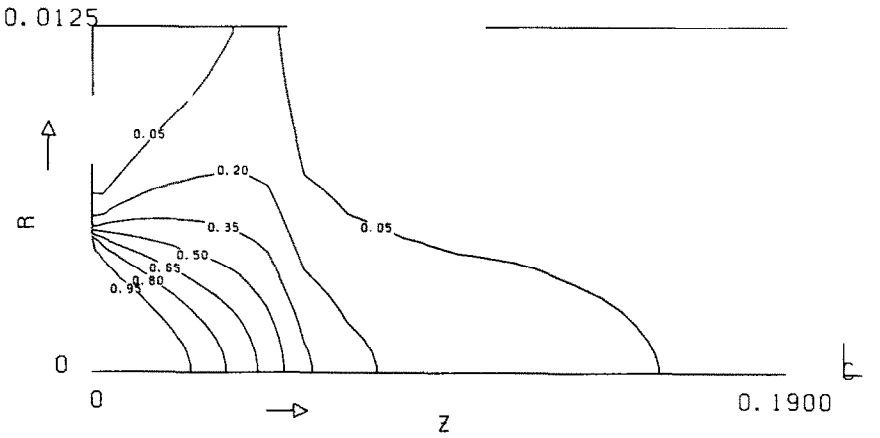

FIG. 6(b). Computed map of argon concentration for sideways injection and $S = 0.5$.

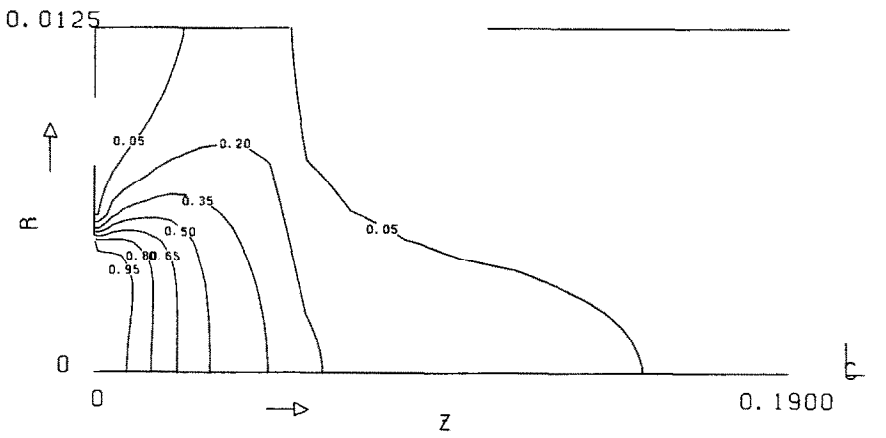

FIG. 6(c). Computed map of argon concentration for sideways injection and $S = 1$.

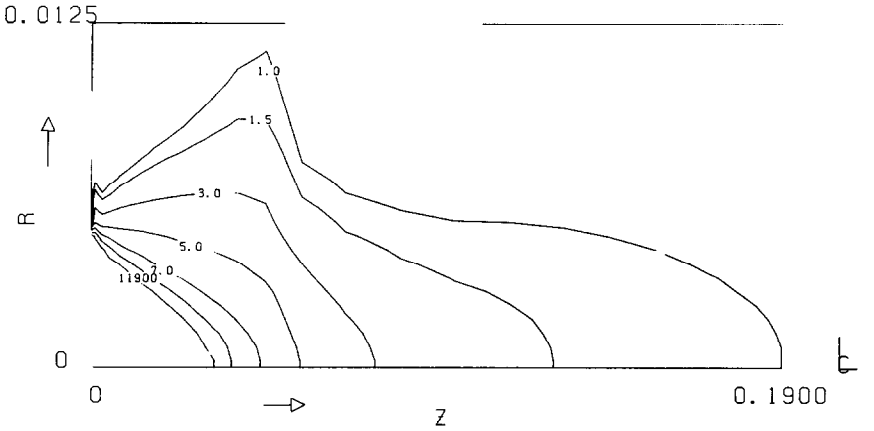

FIG. 7(a). Computed temperature field for sideways injection and $S = 0$.

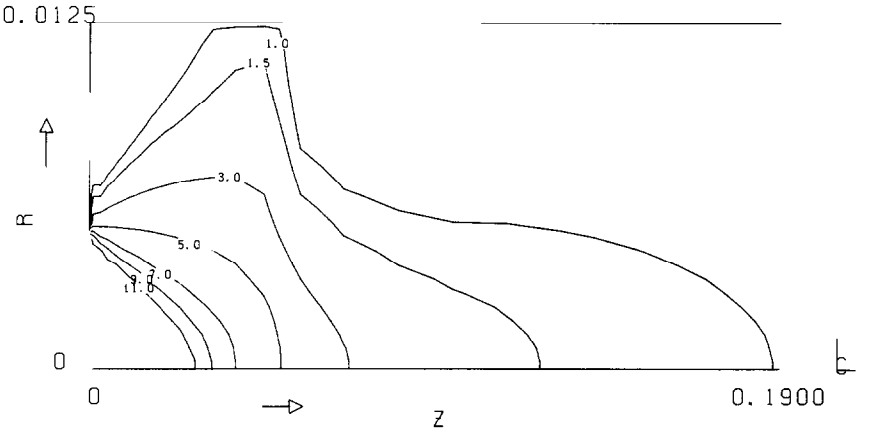

FIG. 7(b). Computed temperature field for sideways injection and $S = 0.5$.

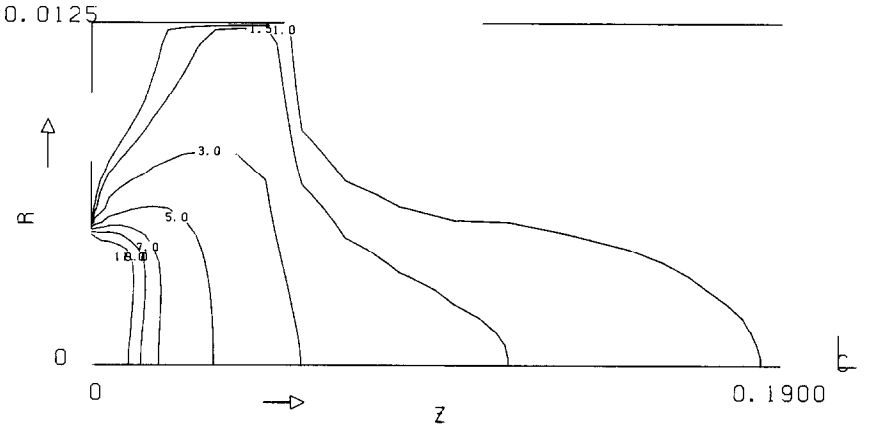

FIG. 7(c). Computed temperature field for sideways injection and $S = 1$.

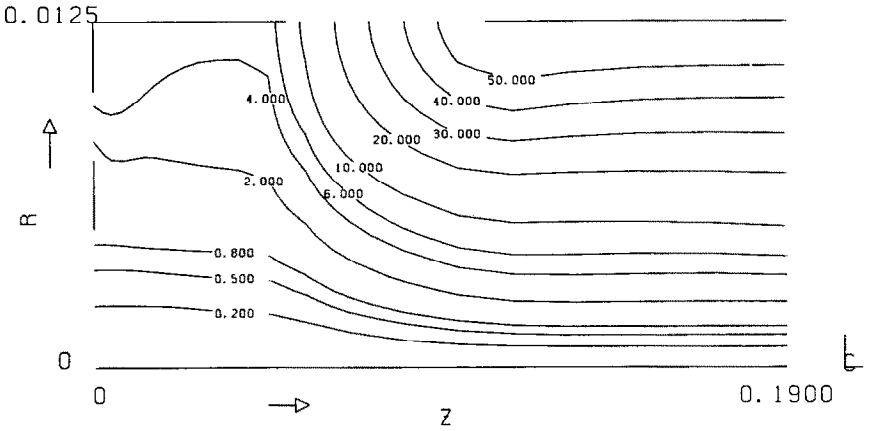

FIG. 8(a). Computed streamline pattern for sideways injection and $S = 0$.

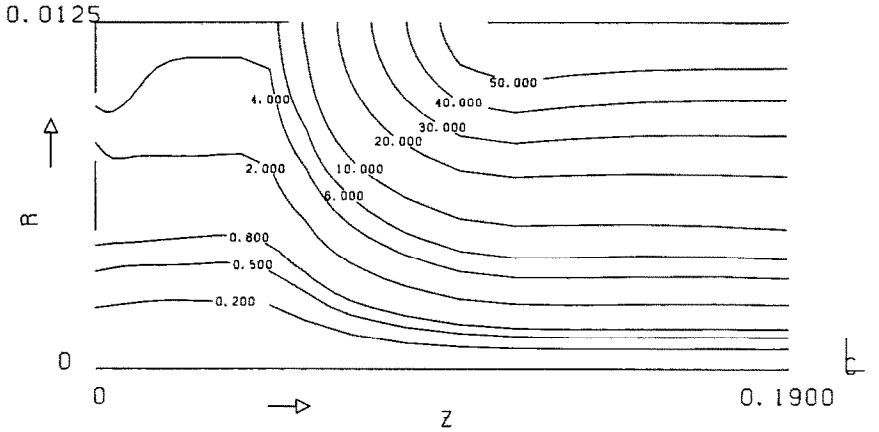

FIG. 8(b). Computed streamline pattern for sideways injection and $S = 0.5$.

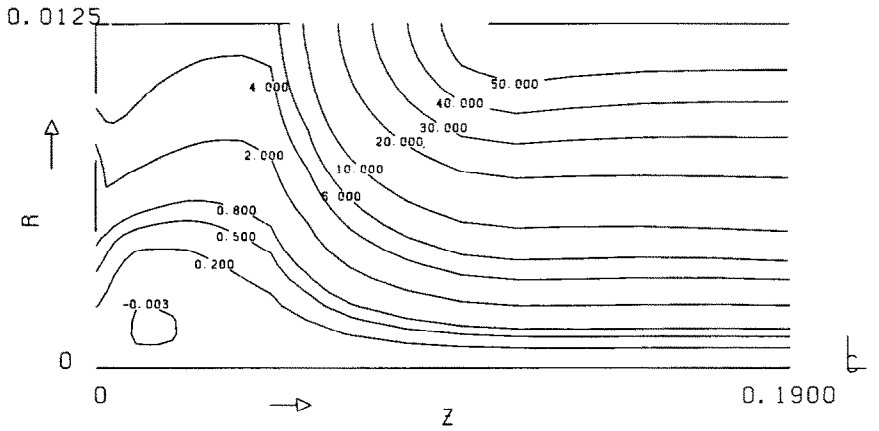

FIG. 8(c). Computed streamline pattern for sideways injection and $S = 1$.

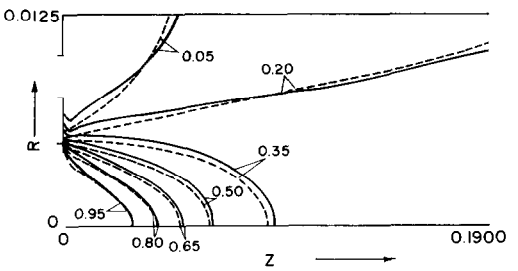

FIG. 9. Computed argon isopleths for both the 'standard case' and the case with a 45° inclination of stream injection through the annular port.

concentration isopleths for both the 'standard case' drawn with the full lines, and the case with a 45° inclination of the stream injected through the annular port. It is seen that changing the angle of inclination does modify the argon concentration profiles, although the effect is not anywhere as dramatic as the introduction of swirl.

Ultimately, the purpose of these calculations is to provide a fundamental basis for the design of reactors in plasma synthesis. The potential utility of this approach is illustrated by showing a preliminary set of results where we consider a system identical to that sketched in Fig. 1, but where silane is injected through the annular port, and methane is introduced through the 'sideways' port. The flow rates employed and the other process parameters are summarized in Table 3.

For the purpose of the calculations, we have neglected coupled flux phenomena; it has been assumed that silane decomposes according to the following relationship, whenever the temperature exceeds a threshold value of about 873 K [20–22]:

$$SiH_4(g) \rightarrow Si(s) + 2H_2(g) \quad \Delta H = -30\,\text{kJ mol}^{-1} \tag{10}$$

Table 3. Input parameters used

$P_w = 37\,\text{kW}$
$Q_m = 5.244 \times 10^{-3}\,\text{kg s}^{-1}$
$Q_p = 1.531 \times 10^{-3}\,\text{kg s}^{-1}$
$Q_t = 7.428 \times 10^{-3}\,\text{kg s}^{-1}$
$R_0 = 0.005\,\text{m}$
$R_1 = 0.0075\,\text{m}$
$R_2 = 0.01\,\text{m}$
$R_r = 0.0125\,\text{m}$
$T_{lw} = 0.3\,\text{kK}$
$T_{tw} = 0.3\,\text{kK}$
$T_t = 0.6\,\text{kK}$
$z_1 = 0.05\,\text{m}$
$z_2 = 0.07\,\text{m}$
$z_3 = 0.32\,\text{m}$
$\eta = 62\%$

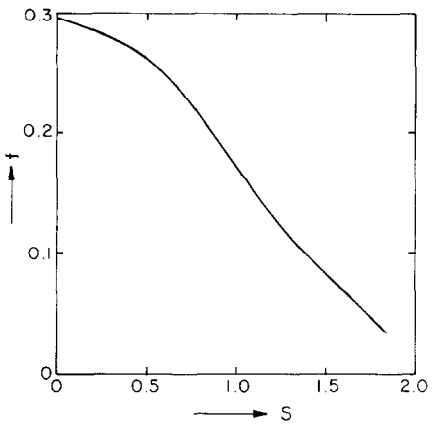

FIG. 10. Computed fraction of unreacted silane at the exit of the ractor as a function of swirl number, S.

with the following Arrhenius-type rate constant:

$$k_t = 2.13 \times 10^{13} \cdot e^{-221(\text{kJ})/RT}\,\text{s}^{-1}. \tag{11}$$

For the time being, methane has been considered as an inert quench gas, which is an oversimplification to be relaxed in the subsequent portion of the study.

Figure 10 shows the fraction of silane unreacted at the exit as a function of the swirl number; it is readily seen that swirl has a profound effect on the performance of the unit. In the present case, the higher swirl number will provide better mixing and more complete conversion. Additional parametric studies could be conducted examining in the first phase:

(a) the combination of process parameters needed to attain complete conversion of the silane,

and in the second phase address:

(b) the design criteria needed to bring about the production of monosized fine particles, e.g. through providing both high reaction rates near the inlet, and high quench rates subsequently; and

(c) the representation of more complex reaction schemes, e.g. those including carbide formation and the like.

4. CONCLUDING REMARKS

A mathematical representation has been developed to describe the three velocity components and the associated temperature and composition fields in a plasma system, which involves the injection of additional gas streams.

In the presentation of the computed results, emphasis has been placed on providing an improved insight into the relationships between the key process parameters, and on developing a feel for the sensitivity of the system to these variables.

It was found that the extent of swirl plays a dominant role in providing mixing between the plasma jet and a reactant gas stream introduced through an annular port.

It was shown, furthermore, that the model may be used to represent the quenching of the system by an axi-symmetrically introduced gas stream, having a direction perpendicular to the jet axis.

Preliminary calculations have indicated that the model may be used to represent the thermal decomposition of silane, the extent of which was found to depend very markedly on the swirl and should depend also on the system geometry. In the development of the transport equations we assumed turbulent flow, which was fully justified, and used the standard K–ε model to represent the turbulent transport coefficients. It should be remarked here that while the standard K–ε model has been extensively tested for a range of recirculating flows, its validation for swirling flows with steep temperature gradients is less complete. Nevertheless, there is supporting evidence in the combustion and allied literature that swirling flows may be satisfactorily represented by this technique [7, 23–25]. Ongoing experimental work may aid a further critical assessment of these approaches.

It is suggested that the model developed here should form the basis of designing plasma reaction systems where the attainment of the optimal combination of process parameters is critical in obtaining the desired monodispersed fine particles.

Work is continuing in this direction.

Acknowledgements—The authors wish to thank the U.S. Department of Energy for partial support of this investigation under Grant No. DE-FG02-85ER-13331, and the United States Education Foundation in Pakistan and Council for International Exchange of Scholars in Washington, DC.

REFERENCES

1. K. Akashi, S. Ohno, R. Ishizuka and T. Yoshida, The characteristics of titanium microcrystals formed from a mixture of titanium tetrachloride and hydrogen in an argon plasma jet, *Proc. 3rd Int. Symp. on Plasma Chemistry*, Vol. 3, Paper S.4.6 (1977).
2. E. Bourdin and P. Fauchais, Aluminum nitride and silicon nitride synthesis from elements in a nitrogen DC plasma jet, *Proc. 3rd Int. Symp. on Plasma Chemistry*, Vol. 3, Paper G.1 (1977).
3. J. F. Coudert, E. Bourdin and P. Fauchais, Kinetic modelling of the reduction of $SiCl_4$ in an arc heater for the production of silicon, *Plasma Chem. Plasma Process.* **2**(4), 399–419 (1982).
4. P. C. Kong, M. Suzuki, R. Young and E. Pfender, Synthesis of β-WC_{1-x} in an atmospheric-pressure thermal plasma jet reactor, *Plasma Chem. Plasma Process.* **3**(1), 115–133 (1983).
5. J. M. Mexmain, D. Morvan, E. Bourdin, J. Amouroux and P. Fauchais, Thermodynamic study of the ways of preparing silicon, and its application to the preparation of photovoltaic silicon by the plasma technique, *Plasma Chem. Plasma Process.* **3**(4), 393–420 (1983).
6. B. E. Launder and D. B. Spalding, The numerical computation of turbulent flows, *Comp. Meth. Appl. Mech. Engng* **3**, 269–289 (1974).
7. E. E. Khalil, D. B. Spalding and J. H. Whitelaw, The calculation of local flow properties in two-dimensional furnaces, *Int. J. Heat Mass Transfer* **18**, 755–791 (1975).
8. A. S. Novick, G. A. Miles and D. G. Lilley, Numerical simulation of combustor flowfields: a primitive variable design capability, *J. Energy* **3**(2), 95–105 (1979).
9. Y. El-Banhawy and J. H. Whitelaw, Calculation of the flow properties of a confined kerosene-spray flame, *AIAA J.* **18**(2), 1503–1510 (1980).
10. W. P. Jones and J. H. Whitelaw, Calculation methods for reacting flows: a review, *Combust. Flame* **48**, 1–26 (1982).
11. N. A. Chigier and A. Chervinsky, Experimental investigation of swirling vortex motions in jets, *ASME J. Appl. Mech.* **89**, 443–451 (1967).
12. N. A. Chigier and J. M. Beer, Velocity and static pressure distributions in swirling air jet issuing from annular and divergent nozzles, *Trans. Am. Soc. Mech. Engrs*, Series D, *Basic Engng* **86**, 788–796 (1964).
13. W. M. Pun and D. B. Spalding, A general computer program for two-dimensional elliptic flows, Rept No. HTS/76/2, Imperial College of Science and Technology, London (1976).
14. B. E. Launder and D. B. Spalding, *Mathematical Models of Turbulence*. Academic Press, London (1972).
15. A. D. Gosman and W. M. Pun, Calculation of recirculating flows, Rept No. HTS/74/2, Dept. of Mech. Engng, Imperial College, London (1974).
16. S. V. Patankar and D. B. Spalding, A calculation procedure for heat, mass and momentum transfer in three-dimensional parabolic flows, *Int. J. Heat Mass Transfer* **16**, 1787–1806 (1972).
17. L. S. Caretto, A. D. Gosman, S. V. Patankar and D. B. Spalding, Two calculation procedures for steady, three-dimensional flows with recirculation, *Proc. 3rd Int. Conf. on Numerical Methods in Fluid Mechanics*, Vol. II, pp. 60–68 (1973).
18. C. H. Liu, Ph.D. Thesis, Numerical analysis of the anode region of high intensity arcs, Department of Mechanical Engineering, University of Minnesota, Minneapolis (1977).
19. J. M. Yos, Technical Memorandum RAD-TM-63-7, Research and Advanced Development, AVCO Corporation, Wilmington, Massachusetts (1963).
20. R. A. Marra, Homogeneous nucleation and growth of silicon powder from laser heated gas phase reactants, Ph.D. Thesis, Massachusetts Institute of Technology (1983).
21. E. M. Coltrin, J. K. Kee and A. J. Miller, A mathematical model of the coupled fluid mechanics and chemical kinetics in a chemical vapor deposition reactor, *J. Electrochem. Soc. Solid State Sci. Technol.* **131**, 425–434 (1984).
22. I. S. Akmandor, Theoretical and computational models of reacting silane gas flows: laser driven pyrolysis of subsonic and supersonic jets, Ph.D. Thesis, Massachusetts Institute of Technology (1985).
23. I. Kubo and F. C. Gouldin, Numerical calculations of turbulent flows, *ASME J. Fluids Engng* **97**, 310–315 (1975).
24. A. D. Gosman and E. Loannides, Aspects of computer simulation of liquid-fuelled combustors, AIAA Paper No. 81-0323 (1981).
25. R. Boysan, W. H. Ayers, J. Swithebank and Z. Pan, Three-dimensional model of spray combustion in gas-turbine combustors, *J. Energy* **6**, 368–375 (1981).

ECOULEMENT ET TRANSFERT DE CHALEUR DANS LES REACTEURS A PLASMA—I. CALCUL DES PROFILS DE VITESSE, DE TEMPERATURE ET DU MELANGE

Résumé—Une représentation mathématique est développée pour décrire le champ des vitesses et des températures et concentrations associées dans un système de jet plasma avec injection de courant gazeux additionnel. On tient compte du tourbillonnement du jet plasma et un objectif important du travail est d'explorer l'effet de ce tourbillon sur les variables principales du mécanisme. On trouve que le tourbillon joue un rôle important dans le mélange entre le jet plasma et un courant gazeux réactant ou diluant introduit à travers une ouverture annulaire. Le modèle peut être utilisé pour représenter la trempe du système par introduction d'un courant gazeux axisymétrique ayant une direction perpandiculaire à l'axe du jet.

FLUIDSTRÖMUNG UND WÄRMEÜBERGANG IN PLASMAREAKTOREN—I. BERECHNUNG VON GESCHWINDIGKEIT, TEMPERATURPROFIL UND MISCHVORGANG

Zusammenfassung—Zur Beschreibung des Geschwindigkeitsfeldes und der auftretenden Temperatur- und Konzentrationsverteilung in einem Plasmastrahl wurde eine mathematische Darstellung entwickelt, die die Zufuhr zusätzlicher Gasströme berücksichtigt. Bei der Formulierung des Problems wurde die Möglichkeit einer Verwirbelung des Plasmastrahls berücksichtigt. Ein wichtiges Ziel der Untersuchung war die Erklärung der Einflüsse auf die wichtigsten Prozeßgrößen. Es ergab sich, daß die Verwirbelung eine wichtige Rolle bei der Vermischung des Plasmastrahls mit einem Reaktanden oder einem verdünnten Gasstrom spielt, welcher durch einen ringförmigen Spalt eintritt. Weiterhin wurde gezeigt, daß das Modell ebenso zur Darstellung des Abschreckvorganges im System benutzt werden kann. Der Abschreckvorgang wird dabei durch einen achssymmetrisch eintretenden Gasstrom, der rechtwinklig zur Strahlachse liegt, hervorgerufen.

ГИДРОДИНАМИКА И ТЕПЛООБМЕН В ПЛАЗМЕННЫХ РЕАКТОРАХ—I. РАСЧЕТ ПОЛЕЙ СКОРОСТИ, ТЕМПЕРАТУРЫ И СМЕШЕНИЯ

Аннотация—Разработано математическое описание полей скорости, температуры и концентрации в системе плазменных струй с дополнительным вдувом газа. Постановка задачи учитывает закрутку плазменной струи, и одна из главных целей—изучить влияние закрутки на основные характеристики процесса. Найдено, что завихрение играет важную роль для смешения плазменной струи и реагента или газа-разбавителя, вводимого через кольцевое отверстие. Кроме того показано, что модель может использоваться для описания затухания при осесимметричном вдуве газового потока перпендикулярно оси струи.